



**Journal of  
Mechanics of  
Materials and Structures**

**A SIMPLE TECHNIQUE FOR ESTIMATION OF  
MIXED MODE (I/II) STRESS INTENSITY FACTORS**

Soman Sajith, Kondepudi S. R. K. Murthy and Puthuveetil S. Robi

**Volume 13, No. 2**

**March 2018**





## A SIMPLE TECHNIQUE FOR ESTIMATION OF MIXED MODE (I/II) STRESS INTENSITY FACTORS

SOMAN SAJITH, KONDEPUDI S. R. K. MURTHY AND PUTHUVEETIL S. ROBI

A simple and efficient finite element based technique using the crack face nodal displacements for the accurate estimation of mode I, mode II and mixed mode I/II stress intensity factors (SIF) is proposed in this paper. Finite element (FE) method is used to obtain the crack face nodal displacements of various cracked configurations. Convergence studies are conducted. The estimated SIFs are compared with the other techniques such as displacement extrapolation, J-integral, and interaction integral techniques, along with the published results. Results indicate that the proposed technique is found to be simple and provides accurate SIF even for the relatively coarser meshes. Results also indicate that the accuracy of the proposed technique is of the order of the path independent integrals in a given mesh. Further, the proposed technique also evaluates the sign of mode II SIF,  $K_{II}$ , which is vital in fatigue crack growth simulations.

### 1. Introduction

Stress intensity factor (SIF),  $K$ , proposed by Irwin [1957] plays a vital role in the strength and structural integrity assessment of cracked structures. It is used to describe the crack driving force, the level of singularity [Paris 2014], and the materials resistance to fracture. Further, it is also useful in fatigue crack growth studies. To this end, numerous analytical [Sih 1973], experimental [Ravi-Chandar 2008; Swamy et al. 2008; Kaushik et al. 2008], and numerical methods [Henshell and Shaw 1975; Barsoum 1976; Banks-Sills and Sherman 1986; Lim et al. 1992; Mukhopadhyay et al. 2000; Murthy and Mukhopadhyay 2001; Qian et al. 2016; Yan et al. 2010] are available for the SIF determination.

Analytical and semianalytical SIF solutions of some simple configurations are available in various handbooks [Tada et al. 2000; Murakami 1987; Laham 1999]. For complex configurations, numerical methods such as FE method and boundary element (BE) method are employed. Amongst the available numerical methods, FE method has been extensively used for accurately estimating SIFs of complex configurations. Other important areas which demand accurate estimation of the SIFs is FE simulations of quasistatic crack growths and fatigue crack growth in damage tolerance design philosophy. In these studies, a large number of finite element analyses of a given cracked configuration are necessary due to the incremental increase of the crack length. In such cases, it is cost effective if accurate SIFs are estimated for a given mesh in the simulation process. Moreover, the signs of individual SIFs are also important in estimating crack growth directions both in quasistatic and fatigue crack growth simulations.

In FE method, quarter point elements (QPEs) [Henshell and Shaw 1975; Barsoum 1976] are employed at the crack tip for modeling the crack tip inverse square root singularity. In relation to the QPEs and FE method, a number of SIF estimation techniques have also been developed. A review of some of these

---

*Keywords:* crack, stress intensity factor, fracture, fatigue, displacement, mixed mode.

commonly used techniques are available in works [Banks-Sills and Sherman 1986; Lim et al. 1992; Mukhopadhyay et al. 2000; Murthy and Mukhopadhyay 2001; Qian et al. 2016].

SIF estimation techniques (usually postprocessing techniques) are broadly classified into stress-based, displacement-based, and energy-based. The displacement-based techniques include: the limited displacement extrapolation technique by Lim et al. [1992], the displacement correlation technique [Tracey 1977], the displacement extrapolation techniques (DETs) [Chan et al. 1970; Shih et al. 1976; Rahulkumar et al. 1997; Guinea et al. 2000; ANSYS 2007; Kirthan et al. 2016], the quarter point displacement technique [Barsoum 1976; Henshell and Shaw 1975; Lim et al. 1992], and the interior collocation technique [Jogdand and Murthy 2010]. Some of the stress-based methods are the stress extrapolation [Chan et al. 1970] and the force method [Raju and Newman, Jr. 1977]. Examples of energy-based SIF extraction methods are the modified crack closure integral [Ramamurthy et al. 1986; Rybicki and Kanninen 1977; Sethuraman and Maiti 1988], virtual crack closure integral [Rybicki and Kanninen 1977; Shivakumar et al. 1988], J-integral [Rice 1968], stiffness derivative [Parks 1974], virtual crack extension [Hellen 1975], and interaction integral (I-integral) [Nakamura 1991; Shih et al. 1986].

Amongst the above methods, J-integral, interaction integral, and a kind of DET are integrated in various commercial software such as ANSYS and ABAQUS. Although the path independent integral techniques (J-integral and interaction integral) neatly avoid crack tip complications, they only provide accurate solutions of the SIFs by computing over several paths, which complicates the mesh generation process. The interior collocation technique [Jogdand and Murthy 2010], although it provides accurate values of the SIFs, demands a special mesh pattern around the crack tip. As a consequence, these are difficult to implement into the existing FE codes. On the other hand, techniques such as stiffness derivative and virtual crack extension require calculation of the structural stiffness matrix twice, which increases the computational cost. It is evident that the above techniques, apart from being difficult to incorporate into the existing codes, are also not very appropriate for employment in the crack growth simulations where large numbers of analysis steps are usually needed.

While the displacement-based techniques are simple and easy to implement into existing FE codes (they demand no other than quarter point elements), techniques such as displacement correlation [Tracey 1977] and quarter point displacement techniques [Barsoum 1976; Henshell and Shaw 1975; Lim et al. 1992] do not show convergence as the meshes are refined [Murthy and Mukhopadhyay 2001]. Clearly, use of these techniques is prohibitive especially in crack growth simulations. Coming to the case of displacement extrapolation methods, a form of displacement extrapolation was first proposed by Chan et al. [1970], which has the limitation of carrying out regression analysis for best-fit straight line. Subsequently, many variants of displacement extrapolation techniques have been proposed in the past [Shih et al. 1976; Rahulkumar et al. 1997; Guinea et al. 2000; ANSYS 2007; Kirthan et al. 2016].

The above extrapolation methods have been devised based on two types of formulations. In the first type of formulations [Rahulkumar et al. 1997; ANSYS 2007], the crack opening displacement (COD) and crack sliding displacement (CSD) are approximated using the singular solutions and these displacements are approximated using an assumed profile (containing singular and higher-order displacements) fitted to the edges of the finite elements attached to crack flanks. In the second type of formulation, the relative displacement of nodes on one of the two flanks of the crack were expressed in terms of known analytical expressions containing singular and higher-order terms and obtained the SIFs by correlating these expressions with the elemental displacement field [Shih et al. 1976; Guinea et al. 2000; Kirthan et al.

2016]. It has been shown using extensive numerical analyses that the techniques based on the second type of formulation [Shih et al. 1976; Guinea et al. 2000; Kirthan et al. 2016] do not converge as the meshes are refined [Murthy and Mukhopadhyay 2001]. Clearly, these existing displacement techniques are not reliable when estimating SIFs of complex configurations or during fatigue crack propagation simulations. A technique based on the first type of formulation is implemented in commercial software ANSYS, and although it estimates accurate values of the SIFs, it has a major limitation of not providing the signs of the SIFs, which are extremely important in fatigue crack growth simulations.

In view of the importance of accurately estimating SIFs along with their signs and various limitations of the existing SIF extraction methods (as described above), a new simple and efficient displacement extrapolation-type technique, which also provides signs of the estimated SIFs, is proposed in the present investigation. This work takes the advantage of both the types of formulations implemented in the existing techniques [Shih et al. 1976; Zhu and Smith 1995; Rahul Kumar et al. 1997] and formulates the COD and CSD using a combination of singular and higher-order terms. Due to the presence of higher-order terms, the technique can be used on coarse meshes to get the accurate values of SIFs. The mixed mode SIFs are then estimated directly by comparing the analytical expressions of COD and CSD with the computed values obtained at the nodes of the crack flanks. Further, the proposed technique employs the more elegant approach of the Generalized Westergaard proposed by Sanford [1979]. It is very easy to implement into the existing FE codes and provides very accurate SIFs even in the relatively course meshes. The solutions of the proposed technique converge as the meshes are refined. The efficacy of the proposed technique is substantiated by solving the SIFs of mode I, mode II, and mixed mode (I/II) benchmark problems and comparing the results with the values computed using J-integral and interaction integral and published results.

The organization of the paper is as follows. Section 2 describes the mathematical background and implementation steps of the proposed technique. Numerical validation of the proposed technique using benchmark problems is presented in Section 3. Finally, Section 4 presents the summary and conclusions.

## 2. Theoretical background

In the generalized Westergaard method [Sanford 1979], the modified Airy stress function for opening mode ( $\phi_I$ ) and shear mode ( $\phi_{II}$ ) are respectively given by

$$\phi_I = \text{Re}\bar{\bar{Z}}_I(z) + y\text{Im}\bar{\bar{Z}}_I(z) + y\text{Im}\bar{Y}_I(z), \quad \phi_{II} = -y\text{Re}\bar{Z}_{II}(z) + \text{Im}\bar{Y}_{II}(z) - y\text{Re}\bar{Y}_{II}(z), \quad (1)$$

where

$$\frac{d\bar{\bar{Z}}_i}{dz} = \bar{\bar{Z}}_i, \quad \frac{d\bar{Z}_i}{dz} = Z_i, \quad i = I, II. \quad (2)$$

The complex analytic functions for opening mode ( $Z_I(z)$ ,  $Y_I(z)$ ) and those for shearing mode ( $Z_{II}(z)$ ,  $Y_{II}(z)$ ) are defined as

$$\begin{aligned} Z_I(z) &= \sum_{n=0}^{\infty} A_n Z^{n-1/2} \quad \text{and} \quad Y_I(z) = \sum_{m=0}^{\infty} B_m Z^m, \\ Z_{II}(z) &= \sum_{n=0}^{\infty} C_n Z^{n-1/2} \quad \text{and} \quad Y_{II}(z) = \sum_{m=0}^{\infty} D_m z^m. \end{aligned} \quad (3)$$

These are series-type functions in terms of the complex variable  $z = x + iy$  ( $z = x \cos \theta + iy \sin \theta$  in polar coordinates; see Figure 1) containing an infinite number of opening mode and shear mode ( $A_0, A_1, \dots, A_\infty; B_0, B_1, \dots, B_\infty$ ) and shear coefficients ( $C_0, C_1, \dots, C_\infty; D_0, D_1, \dots, D_\infty$ ). These coefficients are functions of the geometry and boundary conditions of a cracked configuration. Using Cauchy–Riemann relations and the modified Airy stress function (1), the stress components for mode I in the absence of body forces can be written as

$$\begin{Bmatrix} \sigma_{xx} \\ \sigma_{yy} \\ \tau_{xy} \end{Bmatrix} = \begin{Bmatrix} \operatorname{Re}Z_I - y\operatorname{Im}Z'_I - y\operatorname{Im}Y'_I + 2\operatorname{Re}Y_I \\ \operatorname{Re}Z_I + y\operatorname{Im}Z'_I + y\operatorname{Im}Y'_I \\ y\operatorname{Re}Z'_I - y\operatorname{Re}Y'_I - \operatorname{Im}Y_I \end{Bmatrix}, \quad (4)$$

and the stress components for mode II can be written as

$$\begin{Bmatrix} \sigma_{xx} \\ \sigma_{yy} \\ \tau_{xy} \end{Bmatrix} = \begin{Bmatrix} y\operatorname{Re}Z'_{II} + 2\operatorname{Im}Z_{II} + y\operatorname{Re}Y'_{II} + \operatorname{Im}Y_{II} \\ -y\operatorname{Re}Z'_{II} - y\operatorname{Re}Y'_{II} + \operatorname{Im}Y_{II} \\ \operatorname{Re}Z_{II} - y\operatorname{Im}Z'_{II} - y\operatorname{Im}Y'_{II} \end{Bmatrix}. \quad (5)$$

Integrating the strain components, the displacement components in terms of three parameters ( $A_0, A_1$ , and  $B_0$ ) for mode I can be shown to be

$$\begin{aligned} u^I &= \frac{A_0}{2G} r^{1/2} [(\kappa - 1) \cos \frac{1}{2}\theta + \sin \theta \sin \frac{1}{2}\theta] \\ &\quad + \frac{A_1}{2G} r^{3/2} [\frac{1}{3}(\kappa - 1) \cos \frac{3}{2}\theta - \sin \theta \sin \frac{1}{2}\theta] + \frac{B_0(\kappa + 1)}{4G} r \cos \theta, \\ v^I &= \frac{A_0}{2G} r^{1/2} [(\kappa + 1) \sin \frac{1}{2}\theta - \sin \theta \cos \frac{1}{2}\theta] \\ &\quad + \frac{A_1}{2G} r^{3/2} [\frac{1}{3}(\kappa + 1) \sin \frac{3}{2}\theta - \sin \theta \cos \frac{1}{2}\theta] - \frac{B_0 v(\kappa + 1)}{4G} r \sin \theta, \end{aligned} \quad (6)$$

where  $u^I$  and  $v^I$  represent the mode I displacements in  $x$  and  $y$  directions, respectively (Figure 1) and  $\kappa = 3 - 4\nu$  for plane strain and  $(3 - \nu)/(1 + \nu)$  for plane stress conditions. In a similar way the displacement components in terms of three parameters ( $C_0, C_1$  and  $D_0$ ) for mode II can be obtained as

$$\begin{aligned} u^{II} &= \frac{C_0}{2G} r^{1/2} [(\kappa + 1) \sin \frac{1}{2}\theta + \sin \theta \cos \frac{1}{2}\theta] \\ &\quad + \frac{C_1}{2G} r^{3/2} [\frac{1}{3}(\kappa + 1) \sin \frac{3}{2}\theta + \sin \theta \cos \frac{1}{2}\theta] + \frac{D_0(\kappa + 1)}{4G} 4 \sin \theta, \\ v^{II} &= \frac{C_0}{2G} r^{1/2} [(1 - \kappa) \cos \frac{1}{2}\theta + \sin \theta \sin \frac{1}{2}\theta] \\ &\quad + \frac{C_1}{2G} r^{3/2} [\frac{1}{3}(1 - \kappa) \cos \frac{3}{2}\theta - \sin \theta \sin \frac{1}{2}\theta] - \frac{D_0(\kappa + 1)}{4G} 4 \cos \theta, \end{aligned} \quad (7)$$

where  $u^{II}, v^{II}$  are mode II displacements (Figure 1). Here,  $G$  and  $\nu$  are the shear modulus and Poisson's ratio, respectively. Also,  $A_0, A_1, B_0$  and  $C_0, C_1, D_0$  represent coefficients of the Generalized Westergaard [Sanford 1979] in mode I and mode II, respectively. In the case of mixed mode (I/II) loading, the displacement components can be obtained using the principle of superposition as

$$u = u^I + u^{II}, \quad v = v^I + v^{II}. \quad (8)$$

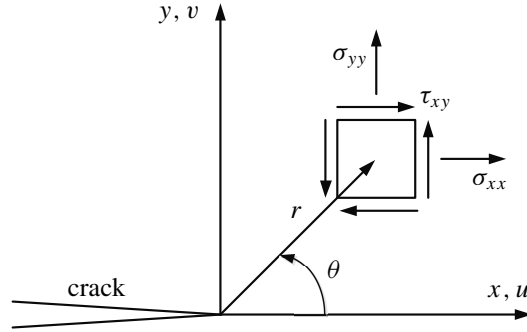


**Figure 1.** Crack tip coordinate system.

Figure 2 shows a typical crack tip mesh pattern with the QPEs deployed at the crack tip. The nodes 1 and 2 represent quarter point nodes on the crack flanks (with node 1 being at  $\theta = +180^\circ$  and node 2 at  $\theta = -180^\circ$ , respectively), and nodes 3 and 4 represent corner nodes of the QPEs attached to the crack flanks. It is assumed that (7) and (8) are sufficient to represent the displacement components along the length of the QPEs lying on the crack flanks in any loading. Referring to Figure 2, for  $\theta = \pm 180^\circ$  the  $v$  component of the displacement in mixed mode loading conditions is given as

$$\begin{aligned} v_{180^\circ} &= \frac{A_0(\kappa+1)}{2G} r^{1/2} - \frac{A_1(\kappa+1)}{6G} r^{3/2} + \frac{D_0(\kappa+1)}{4G} r, \\ v_{-180^\circ} &= -\frac{A_0(\kappa+1)}{2G} r^{1/2} + \frac{A_1(\kappa+1)}{6G} r^{3/2} + \frac{D_0(\kappa+1)}{4G} r. \end{aligned} \quad (9)$$

Similarly the  $u$  component of the displacement is given as

$$\begin{aligned} u_{180^\circ} &= \frac{C_0(\kappa+1)}{2G} r^{1/2} - \frac{C_1(\kappa+1)}{6G} r^{3/2} - \frac{B_0(\kappa+1)}{4G} r, \\ u_{-180^\circ} &= -\frac{C_0(\kappa+1)}{2G} r^{1/2} + \frac{C_1(\kappa+1)}{6G} r^{3/2} - \frac{B_0(\kappa+1)}{4G} r. \end{aligned} \quad (10)$$

Therefore, from (9) and (10), the COD ( $\Delta v$ ) and CSD ( $\Delta u$ ) under mixed mode I/II can be written as

$$\begin{aligned} \Delta v &= v_{180^\circ} - v_{-180^\circ} = \frac{A_0(\kappa+1)}{G} r^{1/2} - \frac{A_1(\kappa+1)}{3G} r^{3/2}, \\ \Delta u &= u_{180^\circ} - u_{-180^\circ} = \frac{C_0(\kappa+1)}{G} r^{1/2} - \frac{C_1(\kappa+1)}{3G} r^{3/2}. \end{aligned} \quad (11)$$

In the present investigation the unknown coefficients  $A_0$  and  $C_0$  are solved using the FE solutions of  $\Delta v$  and  $\Delta u$  at two different radial locations  $r_1$  (or  $r_2$ ) and  $r_3$  (or  $r_4$ ) on the crack flank as shown in Figure 2. Then the mixed mode SIFs  $K_I$  and  $K_{II}$  can be estimated as

$$K_I = \sqrt{2\pi} A_0 \quad \text{and} \quad K_{II} = \sqrt{2\pi} C_0. \quad (12)$$

It can be noticed from (11) and (12) that actual signs (positive or negative) of the SIFs (which depend on the orientation of the crack with the loading) can also be furnished by the proposed technique.

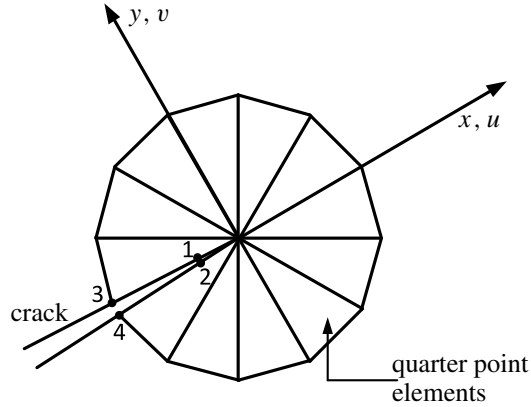


**Figure 2.** Crack tip coordinate system and associated displacements.

### 3. Numerical examples

In order to validate the performance of the proposed technique, numerical evaluation is carried out in this section using a number of benchmark problems. Finite element analysis of all the examples is carried out using the commercial software ANSYS. Meshing is done using eight noded isoparametric quadrilateral (Q8) elements and collapsed Q8 QPEs are employed at the crack tip in a spider web pattern. Plane stress condition, Young's modulus  $E = 1.0$ , Poisson's ratio  $\nu = 0.3$ , and the applied stress  $\sigma = 1.0$  are assumed in all the example problems. Units of all examples are consistent. SIFs are also computed using the DET available in ANSYS, the J-integral and I-integral techniques. In order to study the efficacy of the proposed technique, these values along with the published solutions are compared with those obtained using the present technique. The percentage relative error in the estimated SIF is calculated as

$$\% \text{ relative error} = \left| \frac{\text{computed value} - \text{reference value}}{\text{reference value}} \right| \times 100, \quad (13)$$

where computed value refers to the value of SIF estimated using the proposed technique and the reference value is the available analytical or numerical value.

**3.1. Example 1: center-cracked plate subjected to uniform tension.** The first example discussed here is a mode I problem of a center-cracked plate (CCP) under uniform tensile loading (Figure 3a) with  $h/b = 3$ . Three configurations with  $a/b = 0.2, 0.4$  and  $0.6$  have been considered for the study. Due to symmetry, only one quarter of the CCP is simulated (shaded area in Figure 3a). Figure 3a also shows symmetry boundary conditions used in the FE analysis. Figure 4 shows a sequence of finite element meshes employed for convergence study for the configuration with  $a/b = 0.4$  and with the QPE length to crack length ratio ( $L_Q/a$ ) of  $0.4, 0.2,$  and  $0.1,$  respectively. The number of elements (NE) and number of nodes (NN) are also shown in Figure 4. The mesh pattern around the crack tip is shown in Figure 4d.

Table 1 shows the results of the estimated normalized SIF obtained using the proposed approach and other techniques. The values given in parentheses indicates the percentage relative error based on the reference solutions given by Isida [1971] in (13).

It can be noticed from Table 1 that the results obtained using the proposed technique converges to the reference value with the mesh refinement. This is true for all  $a/b$  values considered. It is interesting to



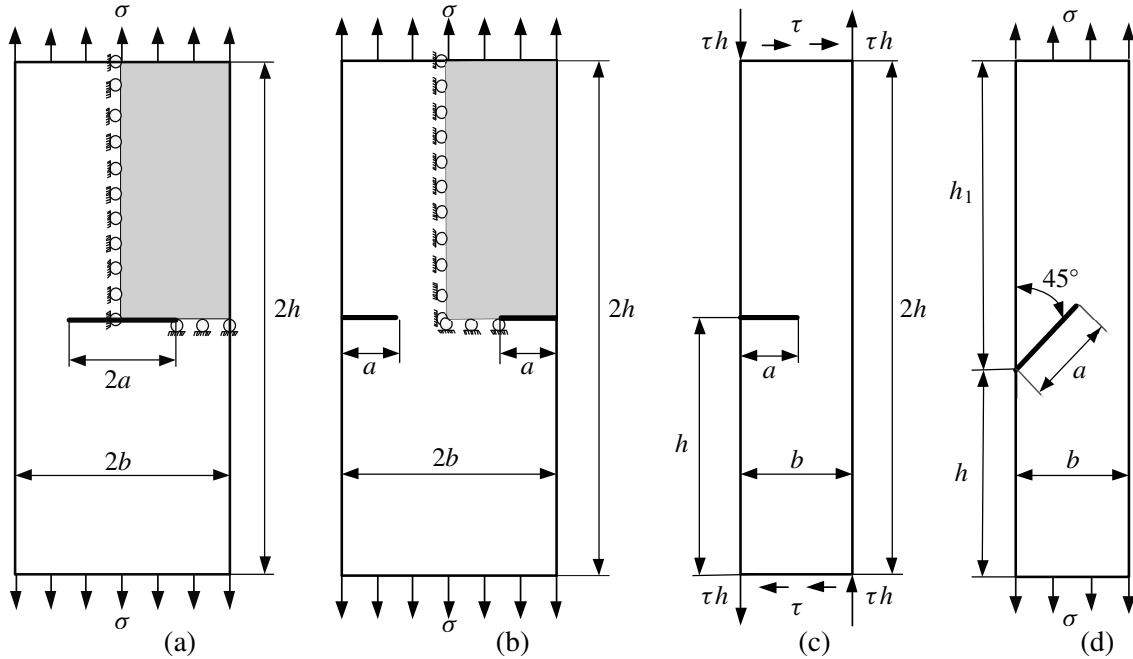


**Figure 3.** Geometry and boundary conditions for the various crack configurations.

$a/b$	Mesh	$K_I/\sigma\sqrt{\pi a}$				
		[Isida 1971]	Present	DET	J-int	I-int
0.2	Mesh 1		1.0272 (0.21)	1.0272 (0.22)	1.0246 (0.04)	1.0249 (0.01)
	Mesh 2	1.025	1.0263 (0.13)	1.0264 (0.13)	1.0246 (0.04)	1.0246 (0.04)
	Mesh 3		1.0258 (0.08)	1.0258 (0.07)	1.0246 (0.04)	1.0246 (0.04)
0.4	Mesh 1		1.1120 (0.27)	1.1120 (0.27)	1.1094 (0.03)	1.1097 (0.06)
	Mesh 2	1.109	1.1109 (0.17)	1.1109 (0.17)	1.1094 (0.03)	1.1093 (0.03)
	Mesh 3		1.1105 (0.14)	1.1105 (0.14)	1.1094 (0.03)	1.1093 (0.03)
0.6	Mesh 1		1.3052 (0.17)	1.3052 (0.17)	1.3033 (0.02)	1.3037 (0.05)
	Mesh 2	1.303	1.3047 (0.13)	1.3046 (0.13)	1.3033 (0.02)	1.3033 (0.02)
	Mesh 3		1.3044 (0.11)	1.3045 (0.12)	1.3033 (0.02)	1.3033 (0.02)

**Table 1.** Comparison of normalized SIFs for CCP ( $h/b = 3$ ,  $a/b = 0.2, 0.4, 0.6$ ). Numbers in parentheses are the percentage relative error.

notice from the results in Table 1 that in all the meshes, the SIFs are determined with an accuracy that is comparable with that obtained using J-integral and I-integral. Very accurate SIFs are estimated using the proposed technique even in the relatively course meshes. The maximum percentage error observed using coarse meshes (Mesh 1) is 0.27% and using fine meshes (Mesh 3) is 0.14%. It can also be noticed that the results obtained in this section are in excellent agreement with the reference value and the proposed technique computes very accurate values of the SIFs.

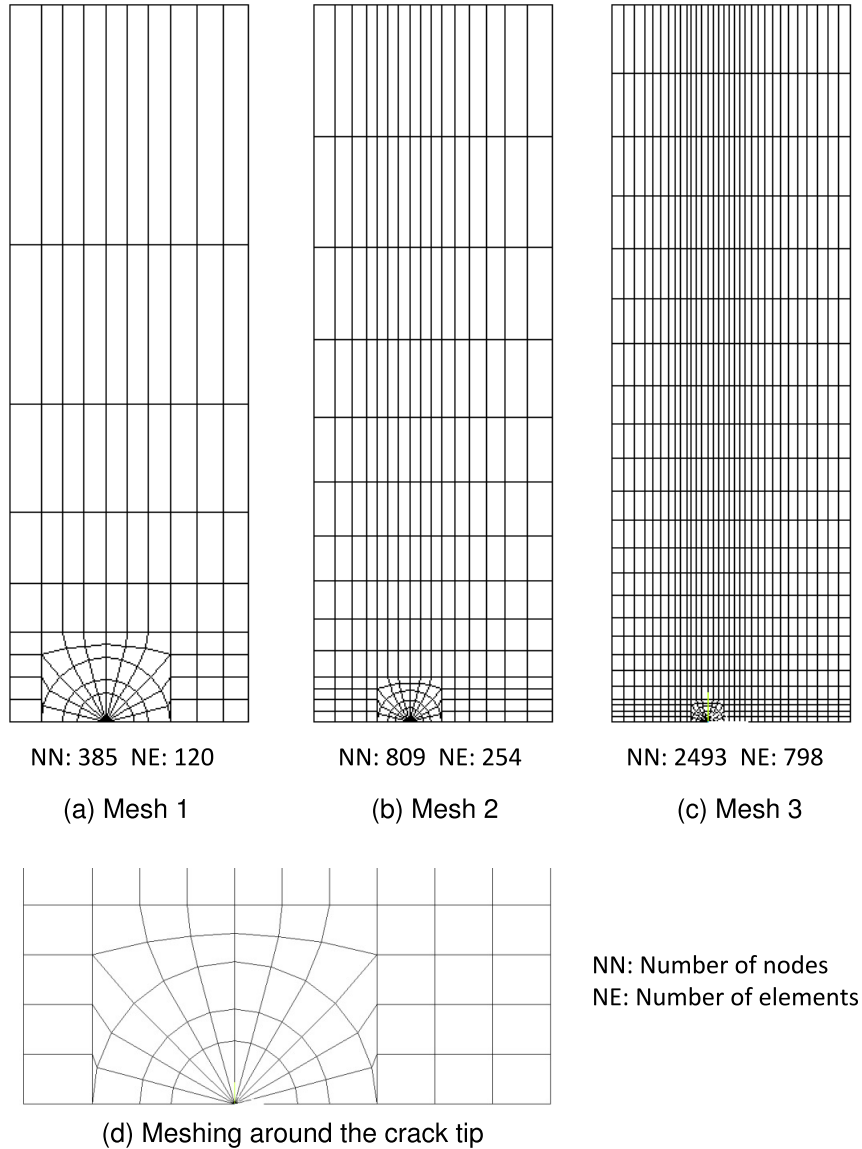


**Figure 4.** Different finite element meshes used for the analysis of CCP. Top: Mesh 1, Mesh 2, and Mesh 3. Bottom: meshing around the tip.

**3.2. Example 2: double edge cracked plate subjected to uniform tension.** The second problem considered is also a mode I problem of double edge cracked plate (DECP) subjected to uniform far-field tensile stresses as shown in Figure 3b. The geometry parameters used for the FE analysis are  $h/b = 3$ ,  $a/b = 0.2, 0.4, \text{ and } 0.6$ . Only one quarter of the plate is modeled as shown (with boundary conditions) in Figure 3b due to the symmetry of the problem. Meshes that are similar to Figure 4 are employed for the FE analysis. However, results corresponding to the Mesh 1 and Mesh 3 are presented here. Table 2 shows

$a/b$	Mesh	$K_I/\sigma\sqrt{\pi a}$					
		Reference 1	Reference 2	Present	DET	J-int	I-int
0.2	Mesh 1	1.1180	1.1123	1.1104 (0.68)	1.1105 (0.67)	1.1118 (0.56)	1.1121 (0.53)
	Mesh 3			1.1124 (0.50)	1.1124 (0.50)	1.1118 (0.56)	1.1117 (0.56)
0.4	Mesh 1	1.1361	1.1377	1.1309 (0.46)	1.1309 (0.46)	1.1321 (0.35)	1.1325 (0.32)
	Mesh 3			1.1329 (0.28)	1.1329 (0.28)	1.1321 (0.35)	1.1321 (0.35)
0.6	Mesh 1	1.2333	1.2446	1.2361 (0.23)	1.2362 (0.23)	1.2360 (0.22)	1.2364 (0.25)
	Mesh 3			1.2371 (0.30)	1.2371 (0.30)	1.2360 (0.22)	1.2360 (0.22)

**Table 2.** Comparison of normalized SIFs for DECP ( $h/b = 3$ ,  $a/b = 0.2, 0.4, 0.6$ ). Reference 1 is [Benthem and Koiter 1973], and reference 2 is [Yan et al. 2010]. Numbers in parentheses are the percentage relative error.

the comparison of computed mode I normalized SIFs using the proposed approach and other techniques. The % relative error is shown in parentheses. Solutions of [Benthem and Koiter 1973] are considered as the reference solution in (13).

It is seen that the results of present displacement based method are in very good agreement with the results using the other three methods and the published results in all the meshes. Like in the previous example, the estimated SIF is converged as the meshes are refined and very accurate solutions are determined even in relatively coarse meshes such as Mesh 1. This is true for all  $a/b$  values considered. The solutions of the proposed technique are comparable to that of path independent integral techniques. The maximum error using Mesh 1 is 0.68%, and that in Mesh 3 is 0.56%.

**3.3. Example 3: edge-cracked plate subjected to pure antisymmetric loading.** In this section, a pure mode II problem of an edge-cracked plate under antisymmetric loading is presented as shown in Figure 3c. For this problem  $h/b$  is set to 1.0 and different configurations with  $a/b = 0.2, 0.4$ , and 0.6 have been analyzed. As no symmetry exists in this problem, the full model is considered in FE analysis. The bottom edge of the plate is restrained from all degrees of freedom and the top face is loaded with the forces as shown in Figure 3c. Like in previous examples, the convergence of computed mode II SIF  $K_{II}$  using the proposed technique is observed along three meshes with varying mesh density as shown in Figure 5 and the corresponding results are presented in Table 3. For the % relative error calculations in normalized SIF, results of [Treifi et al. 2008] are considered as the reference solution.

It may be observed from the results of Table 3 that similar to the previous example, extremely accurate values of the mode II SIFs are extracted by the proposed method and are converged as the meshes are refined. This can be seen in all  $a/b$  values employed. The results obtained using Mesh 3 are in very good agreement with the published results as well as with the other methods. In this example also the accuracy of the proposed method is similar to the J-integral and I-integral techniques. A maximum error of 0.56% is noticed in Mesh 1 of  $a/b = 0.4$ . However with the fine meshes (Mesh 3), the maximum error is 0.51%.

**3.4. Example 4: slant edge cracked plate subjected to tensile loads.** Finally, to demonstrate the efficacy of the proposed method in mixed mode (I/II) loading conditions, a slant edge cracked plate (SECP)

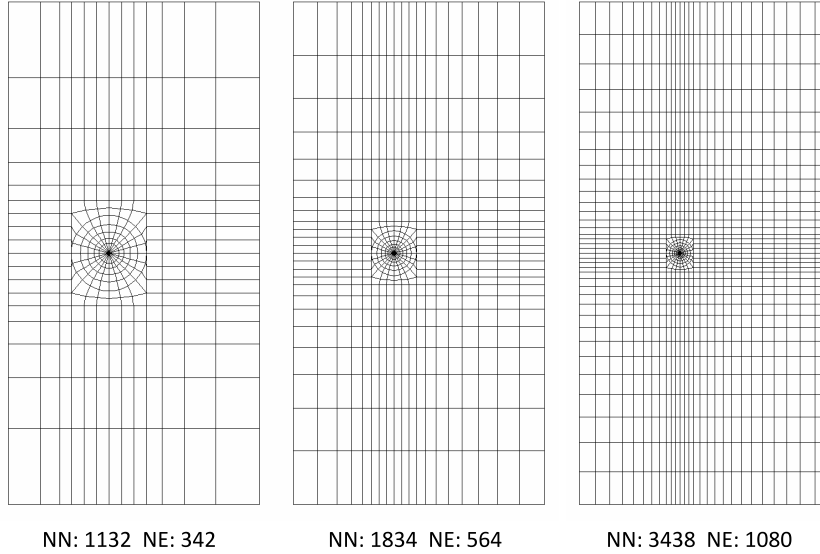


**Figure 5.** Finite element meshes used for analysis of ECP under mode II loading: Mesh 1 (left), Mesh 2 (middle), and Mesh 3 (right).

$a/b$	Mesh	$K_{II}/\tau\sqrt{\pi a}$				
		[Treifi et al. 2008]	Present	DET	J-int	I-int
0.2	Mesh 1		0.6906 (0.49)	0.6906 (0.49)	0.7065 (1.79)	0.7039 (1.43)
	Mesh 2	0.694	0.6887 (0.77)	0.6883 (0.82)	0.6960 (0.29)	0.6960 (0.29)
	Mesh 3		0.6905 (0.51)	0.6905 (0.50)	0.6959 (0.27)	0.6959 (0.27)
0.4	Mesh 1		1.1718 (0.56)	1.1718 (0.56)	1.1794 (0.03)	1.1798 (0.06)
	Mesh 2	1.179	1.1739 (0.40)	1.1740 (0.38)	1.1794 (0.03)	1.1794 (0.03)
	Mesh 3		1.1748 (0.33)	1.1752 (0.29)	1.1794 (0.03)	1.1794 (0.03)
0.6	Mesh 1		1.5468 (0.33)	1.5466 (0.34)	1.5503 (0.11)	1.5507 (0.08)
	Mesh 2	1.552	1.5469 (0.32)	1.5471 (0.31)	1.5509 (0.07)	1.5509 (0.07)
	Mesh 3		1.5474 (0.29)	1.5473 (0.30)	1.5510 (0.06)	1.5510 (0.06)

**Table 3.** Normalized mode II stress intensity factors for ECP ( $h/b = 1$ ,  $a/b = 0.2, 0.4, 0.6$ ). Numbers in parentheses are the percentage relative error.

subjected to tension loads (as shown in Figure 3d) is considered here. The geometric parameters for this problem are  $h/b = 1.0$ ,  $h_1/h = 1.5$ , and  $a/b = 0.3, 0.4, 0.6$ . Due to lack of symmetry, the whole domain is modeled using finite elements. The bottom face of the plate is restrained in the  $x$  and  $y$  directions and the top face is loaded as shown in Figure 3d. The convergence study has also been carried out using the three meshes with varying mesh density as shown in Figure 6. Tables 4 and 5 show the results of the analyses for the normalized  $K_I$  and  $K_{II}$ , respectively.

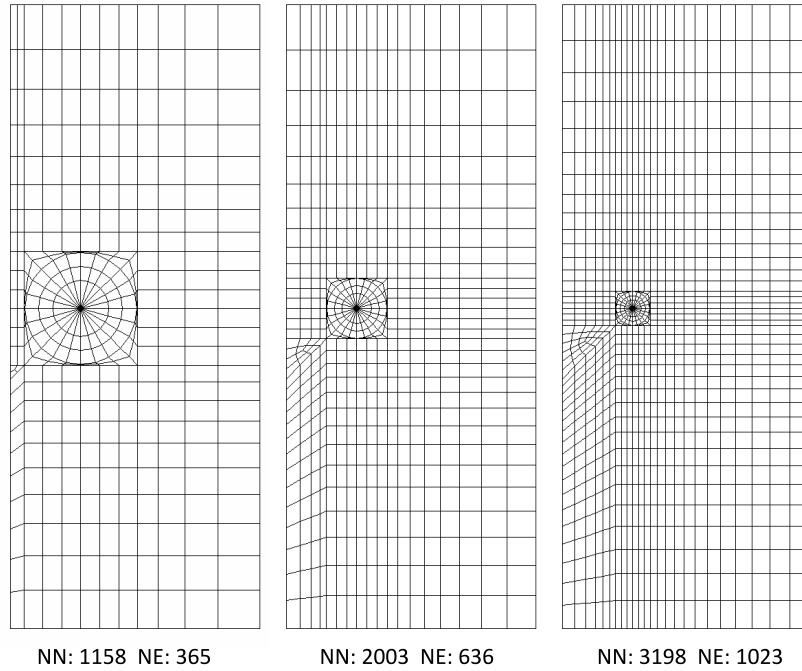


**Figure 6.** Finite element meshes used for the analysis of SECP under tension: Mesh 1 (left), Mesh 2 (middle), and Mesh 3 (right).

$a/b$	Mesh	$K_I/\sigma\sqrt{\pi a}$				
		[Chen and Wang 2008]	[Wilson 1969]	Present	DET	I-int
0.3	Mesh 1			0.8811 (0.21)	0.8811 (0.22)	0.8828 (0.02)
	Mesh 2	0.883	0.883	0.8821 (0.10)	0.8826 (0.05)	0.8826 (0.04)
	Mesh 3			0.8830 (0.00)	0.8831 (0.01)	0.8826 (0.04)
0.4	Mesh 1			1.0155 (0.15)	1.0155 (0.15)	1.0177 (0.07)
	Mesh 2	1.017	1.011	1.0175 (0.05)	1.0177 (0.07)	1.0176 (0.06)
	Mesh 3			1.0178 (0.08)	1.0179 (0.09)	1.0177 (0.07)
0.6	Mesh 1			1.4584 (0.04)	1.4584 (0.04)	1.4590 (0.00)
	Mesh 2	1.459	1.437	1.4595 (0.03)	1.4596 (0.04)	1.4590 (0.00)
	Mesh 3			1.4596 (0.04)	1.4598 (0.05)	1.4590 (0.00)

**Table 4.** Normalized mode I stress intensity factors for SECP under tension ( $h/b = 1$ ,  $h_1/h = 1.5$ ,  $a/b = 0.3, 0.4, 0.6$ ). Numbers in parentheses are the percentage relative error.

It is very interesting to notice from the results of Tables 4 and 5 that like the previous examples, very accurate values of both the SIFs  $K_I$  and  $K_{II}$  have been estimated by the present technique. The percent relative error in present results are of the similar order as that of path independent integrals specifically in the refined meshes. Furthermore, convergence of the extracted SIFs can be noticed from Tables 4 and 5

$a/b$	Mesh	$K_{II}/\sigma\sqrt{\pi a}$				
		[Chen and Wang 2008]	[Wilson 1969]	Present	DET	I-int
0.3	Mesh 1			0.4383 (2.17)	0.4381 (2.20)	0.4469 (0.24)
	Mesh 2	0.448	0.450	0.4423 (1.27)	0.4425 (1.24)	0.4466 (0.30)
	Mesh 3			0.4441 (0.88)	0.4443 (0.84)	0.4466 (0.31)
0.4	Mesh 1			0.4955 (2.28)	0.4955 (2.27)	0.5055 (0.30)
	Mesh 2	0.507	0.505	0.5012 (1.15)	0.5010 (1.19)	0.5051 (0.38)
	Mesh 3			0.5021 (0.98)	0.5020 (0.99)	0.5051 (0.38)
0.6	Mesh 1			0.6782 (1.00)	0.6782 (0.99)	0.6833 (0.24)
	Mesh 2	0.685	0.674	0.6806 (0.64)	0.6805 (0.66)	0.6831 (0.27)
	Mesh 3			0.6807 (0.62)	0.6808 (0.61)	0.6831 (0.27)

**Table 5.** Normalized mode II stress intensity factors for SECP under tension ( $h/b = 1$ ,  $h_1/h = 1.5$ ,  $a/b = 0.3, 0.4, 0.6$ ). Numbers in parentheses are the percentage relative error.

as the meshes are refined. The results in tables clearly show that the proposed technique is capable of providing accurate the mixed mode SIFs even in the relatively coarse meshes similar to that of J- and I-integrals. Solutions of [Chen and Wang 2008] are considered as the reference solutions in (13).

#### 4. Conclusions

A simple and efficient displacement extrapolation technique for estimating mode I, mode II, and mixed mode (I/II) loading conditions is proposed in the present investigation. The technique uses the crack face displacement components from finite element analysis to compute the mode I, mode II, and mixed mode I/II SIFs. The technique is developed based on the Generalized Westergaard approach. The results of the present investigation clearly show that:

- the present technique provides very accurate SIFs even in the relatively coarse meshes,
- the estimated SIFs show convergence as the meshes are refined,
- the estimated SIFs show very good agreement with the published results and those results computed using the J-integral and I-integral, and
- the accuracy of the SIFs estimated using the proposed technique is of similar order as those obtained using path-independent integrals.

Apart from the accuracy of SIFs, another important feature of the proposed technique is that it provides the SIFs with their correct sign, which is vital in fatigue crack growth simulation studies in damage tolerance design philosophy. Thus the present technique is also extremely useful in fatigue crack growth simulations. Owing to the simplicity and ease of implementation, the present method can easily be incorporated into the existing FE codes.

## References

- [ANSYS 2007] “Theory reference manual”, software manual, ANSYS, 2007, Available at <http://www.oalib.com/references/7196604>. Release 11.0.
- [Banks-Sills and Sherman 1986] L. Banks-Sills and D. Sherman, “Comparison of methods for calculating stress intensity factors with quarter-point elements”, *Int. J. Fract.* **32** (1986), 127–140.
- [Barsoum 1976] R. S. Barsoum, “On the use of isoparametric finite elements in linear fracture mechanics”, *Int. J. Numer. Methods Eng.* **10** (1976), 25–37.
- [Benthem and Koiter 1973] J. P. Benthem and W. T. Koiter, *Methods of analysis and solutions of crack problems*, vol. 1, edited by G. C. Sih, Springer, Dordrecht, The Netherlands, 1973.
- [Chan et al. 1970] S. K. Chan, I. S. Tuba, and W. K. Wilson, “On the finite element method in linear fracture mechanics”, *Eng. Fract. Mech.* **2** (1970), 1–17.
- [Chen and Wang 2008] C. H. Chen and C. L. Wang, “Stress intensity factors and T-stresses for offset double edge-cracked plates under mixed-mode loadings”, *Int. J. Fract.* **152** (2008), 149–162.
- [Guinea et al. 2000] G. V. Guinea, J. Planas, and M. Elices, “KI evaluation by the displacement extrapolation technique”, *Eng. Fract. Mech.* **66** (2000), 243–255.
- [Hellen 1975] T. K. Hellen, “On the method of virtual crack extensions”, *Int. J. Numer. Methods Eng.* **9** (1975), 187–207.
- [Henshell and Shaw 1975] R. D. Henshell and K. G. Shaw, “Crack tip finite elements are unnecessary”, *Int. J. Numer. Methods Eng.* **9** (1975), 495–507.
- [Irwin 1957] G. Irwin, “Analysis of stresses and strains near the end of a crack transversing a plate”, *J. Appl. Mech. (ASME)* **24** (1957), 361–370.
- [Isida 1971] M. Isida, “Effect of width and length on stress intensity factors of internally cracked plates under various boundary conditions”, *Int. J. Fract. Mech.* **7** (1971), 301–316.
- [Jogdand and Murthy 2010] P. V. Jogdand and K. S. R. K. Murthy, “A finite element based interior collocation method for the computation of stress intensity factors and T-stresses”, *Eng. Fract. Mech.* **77** (2010), 1116–1127.
- [Kaushik et al. 2008] B. Kaushik, K. S. R. K. Murthy, and P. S. Robi, “Determination of strain gage locations for the accurate measurement of opening mode stress intensity factors”, *J. Mech. Mater. Struct.* **3** (2008), 1757–1771.
- [Kirthan et al. 2016] L. J. Kirthan, R. Hegde, V. A. Girisha, and R. G. Kumar, “Evaluation of mode I stress intensity factor for edge crack using displacement extrapolation method”, *Int. J. Mater. Struct. Integrity* **10** (2016), 11–22.
- [Laham 1999] A. Laham, *Stress intensity factor and limit load handbook*, British Energy Generation Ltd., Gloucester, UK, 1999.
- [Lim et al. 1992] I. L. Lim, I. W. Johnston, and S. K. Choi, “Comparison between various displacement-based stress intensity factor computation techniques”, *Int. J. Fract.* **58** (1992), 193–210.
- [Mukhopadhyay et al. 2000] N. K. Mukhopadhyay, S. K. Maiti, and A. Kakodkar, “A review of SIF evaluation and modelling of singularities in BEM”, *Comput. Mech.* **25** (2000), 358–375.
- [Murakami 1987] Y. Murakami, *Stress intensity factors handbook*, Pergamon, 1987.
- [Murthy and Mukhopadhyay 2001] K. S. R. K. Murthy and M. Mukhopadhyay, “Unification of stress intensity factor (SIF) extraction methods with an h-adaptive finite element scheme”, *Comm. Numer. Methods Engrg.* **17** (2001), 509–520.
- [Nakamura 1991] T. Nakamura, “Three-dimensional stress fields of elastic interface cracks”, *J. Appl. Mech. (ASME)* **58** (1991), 939–946.
- [Paris 2014] P. C. Paris, “A brief history of the crack tip stress intensity factor and its application”, *Meccanica (Milano)* **49** (2014), 759–764.
- [Parks 1974] D. M. Parks, “A stiffness derivative finite element technique for determination of crack tip stress intensity factors”, *Int. J. Fract.* **10** (1974), 487–502.
- [Qian et al. 2016] G. Qian, V. F. González-Albuixech, M. Niffenegger, and E. Giner, “Comparison of KI calculation methods”, *Eng. Fract. Mech.* **156** (2016), 52–67.

- [Rahulkumar et al. 1997] P. Rahulkumar, S. Saigal, and S. Yunus, “Singular p-version finite elements for stress intensity factor computations”, *Int. J. Numer. Methods Eng.* **40** (1997), 1091–1114.
- [Raju and Newman, Jr. 1977] I. S. Raju and J. C. Newman, Jr., “Three dimensional finite-element analysis of finite-thickness fracture specimens”, Technical Report NASA-TN-D-8414, L-10967, NASA Langley Research Center, 1977.
- [Ramamurthy et al. 1986] T. S. Ramamurthy, T. Krishnamurthy, K. B. Narayana, K. Vijayakumar, and B. Dattaguru, “Modified crack closure integral method with quarter point elements”, *Mech. Res. Commun.* **13** (1986), 179–186.
- [Ravi-Chandar 2008] K. Ravi-Chandar, *Springer handbook of experimental solid mechanics*, edited by W. N. Sharpe, Jr., Springer, New York, 2008.
- [Rice 1968] J. R. Rice, “A path independent integral and the approximate analysis of strain concentration by notches and cracks”, *J. Appl. Mech. (ASME)* **35** (1968), 379–386.
- [Rybicki and Kanninen 1977] E. F. Rybicki and M. F. Kanninen, “A finite element calculation of stress intensity factors by a modified crack closure integral”, *Eng. Fract. Mech.* **9** (1977), 931–938.
- [Sanford 1979] R. J. Sanford, “A critical re-examination of the Westergaard method for solving opening-mode crack problems”, *Mech. Res. Commun.* **6** (1979), 289–294.
- [Sethuraman and Maiti 1988] R. Sethuraman and S. K. Maiti, “Finite element based computation of strain energy release rate by modified crack closure integral”, *Eng. Fract. Mech.* **30** (1988), 227–231.
- [Shih et al. 1976] C. F. Shih, H. G. Delorenzi, and M. D. German, “Crack extension modeling with singular quadratic isoparametric elements”, *Int. J. Fract.* **12** (1976), 647–651.
- [Shih et al. 1986] C. F. Shih, B. Moran, and T. Nakamura, “Energy release rate along a three-dimensional crack front in a thermally stressed body”, *Int. J. Fract.* **30** (1986), 79–102.
- [Shivakumar et al. 1988] K. N. Shivakumar, P. W. Tan, and J. C. Newman, “A virtual crack-closure technique for calculating stress intensity factors for cracked three dimensional bodies”, *Int. J. Fract.* **36** (1988), 43–50.
- [Sih 1973] G. C. Sih, *Methods of analysis and solutions of crack problems*, Springer, Dordrecht, 1973.
- [Swamy et al. 2008] S. Swamy, M. V. Srikanth, K. S. R. K. Murthy, and P. S. Robi, “Determination of mode I stress intensity factors of complex configurations using strain gages”, *J. Mech. Mater. Struct.* **3** (2008), 1239–1255.
- [Tada et al. 2000] H. Tada, P. C. Paris, and G. R. Irwin, *The stress analysis of cracks handbook*, ASME Press, New York, 2000.
- [Tracey 1977] D. M. Tracey, “Discussion of “on the use of isoparametric finite elements in linear fracture mechanics” by R. S. Barsoum”, *Int. J. Numer. Methods Eng.* **11** (1977), 401–402.
- [Treifi et al. 2008] M. Treifi, S. O. Oyadiji, and D. K. L. Tsang, “Computations of modes I and II stress intensity factors of sharp notched plates under in-plane shear and bending loading by the fractal-like finite element method”, *Int. J. Solids Struct.* **45** (2008), 6468–6484.
- [Wilson 1969] W. K. Wilson, *Combined mode fracture mechanics*, University of Pittsburgh, California, 1969.
- [Yan et al. 2010] X. Yan, B. Liu, and Z. Hu, “SIFs of rectangular tensile sheets with symmetric double edge defects”, *J. Mech. Mater. Struct.* **5** (2010), 795–803.
- [Zhu and Smith 1995] W. Zhu and D. Smith, “On the use of displacement extrapolation to obtain crack tip singular stresses and stress intensity factors”, *Engrg. Fracture Mech.* **51**:3 (1995), 391–400.

Received 28 Jul 2017. Accepted 4 Mar 2018.

SOMAN SAJITH: [s.sajith@iitg.ac.in](mailto:s.sajith@iitg.ac.in)

Department of Mechanical Engineering, Indian Institute of Technology Guwahati, Guwahati, India

KONDEPUDI S. R. K. MURTHY: [ksrkm@iitg.ac.in](mailto:ksrkm@iitg.ac.in)

Department of Mechanical Engineering, Indian Institute of Technology Guwahati, Guwahati, India

PUTHUVEETIL S. ROBI: [psr@iitg.ac.in](mailto:psr@iitg.ac.in)

Department of Mechanical Engineering, Indian Institute of Technology Guwahati, Guwahati, India



# JOURNAL OF MECHANICS OF MATERIALS AND STRUCTURES

msp.org/jomms

Founded by Charles R. Steele and Marie-Louise Steele

## EDITORIAL BOARD

ADAIR R. AGUIAR	University of São Paulo at São Carlos, Brazil
KATIA BERTOLDI	Harvard University, USA
DAVIDE BIGONI	University of Trento, Italy
MAENGHYO CHO	Seoul National University, Korea
HUILING DUAN	Beijing University
YIBIN FU	Keele University, UK
IWONA JASIUKEWICZ	University of Illinois at Urbana-Champaign, USA
DENNIS KOCHMANN	ETH Zurich
MITSUTOSHI KURODA	Yamagata University, Japan
CHEE W. LIM	City University of Hong Kong
ZISHUN LIU	Xi'an Jiaotong University, China
THOMAS J. PENCE	Michigan State University, USA
GIANNI ROYER-CARFAGNI	Università degli studi di Parma, Italy
DAVID STEIGMANN	University of California at Berkeley, USA
PAUL STEINMANN	Friedrich-Alexander-Universität Erlangen-Nürnberg, Germany
KENJIRO TERADA	Tohoku University, Japan

## ADVISORY BOARD

J. P. CARTER	University of Sydney, Australia
D. H. HODGES	Georgia Institute of Technology, USA
J. HUTCHINSON	Harvard University, USA
D. PAMPLONA	Universidade Católica do Rio de Janeiro, Brazil
M. B. RUBIN	Technion, Haifa, Israel

**PRODUCTION** production@msp.org

SILVIO LEVY Scientific Editor

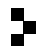
Cover photo: Mando Gomez, [www.mandolux.com](http://www.mandolux.com)

See [msp.org/jomms](http://msp.org/jomms) for submission guidelines.

JoMMS (ISSN 1559-3959) at Mathematical Sciences Publishers, 798 Evans Hall #6840, c/o University of California, Berkeley, CA 94720-3840, is published in 10 issues a year. The subscription price for 2018 is US \$615/year for the electronic version, and \$775/year (+\$60, if shipping outside the US) for print and electronic. Subscriptions, requests for back issues, and changes of address should be sent to MSP.

JoMMS peer-review and production is managed by EditFLOW® from Mathematical Sciences Publishers.

PUBLISHED BY

 **mathematical sciences publishers**  
nonprofit scientific publishing

<http://msp.org/>

© 2018 Mathematical Sciences Publishers

# Journal of Mechanics of Materials and Structures

Volume 13, No. 2

March 2018

---

- A simple technique for estimation of mixed mode (I/II) stress intensity factors**  
SOMAN SAJITH, KONDEPUDI S.R.K. MURTHY and PUTHUVEETIL S. ROBI 141
- Longitudinal shear behavior of composites with unidirectional periodic nanofibers of some regular polygonal shapes**  
HAI-BING YANG, CHENG HUANG, CHUAN-BIN YU and CUN-FA GAO 155
- Fracture initiation in a transversely isotropic solid: transient three dimensional analysis** LOUIS M. BROCK 171
- Eshelby inclusion of arbitrary shape in isotropic elastic materials with a parabolic boundary** XU WANG, LIANG CHEN and PETER SCHIAVONE 191
- Burmister's problem extended to a microstructured layer** THANASIS ZISIS 203
- Multiple crack damage detection of structures using simplified PZT model**  
NARAYANAN JINESH and KRISHNAPILLAI SHANKAR 225



1559-3959(2018)13:2;1-#